

Ethylene hydroformylation on graphite nanofiber supported rhodium catalysts

R. Gao, C.D. Tan, R.T.K. Baker*

Department of Chemistry, Northeastern University, Boston, MA 02115, USA

Abstract

We have investigated the effect of supporting rhodium on several different types of graphite nanofibers (GNFs) for the ethylene hydroformylation reaction at temperatures over the range 180–300°C. The performance of these systems was compared with that of a catalyst where the same metal loading was dispersed on silica. It was found that in general, while the activity of all the catalyst systems was similar, the GNF supported rhodium catalysts exhibited a higher selectivity for the formation of propionaldehyde than the corresponding silica supported system. Furthermore, among the various rhodium/GNF catalysts, the ribbon type nanofibers appeared to give the highest selectivity to the desired product. The optimum temperature for the hydroformylation reaction was found to be 240°C, since at this condition one was able to achieve the combination of maximum activity with acceptable selectivity. Based on many experiments in which the ratio of gaseous reactants was systematically varied it was evident that high partial pressures of CO and C₂H₄, and a concomitant low partial pressure of H₂ gave the optimum performance. It is believed that the morphological characteristics acquired by rhodium when dispersed on the GNF edges is a critical factor rather than the size of the individual crystallites. © 2001 Published by Elsevier Science B.V.

Keywords: Graphite nanofiber supports; Ethylene hydroformylation; Supported rhodium catalysts

1. Introduction

Homogeneous ethylene hydroformylation catalyzed by rhodium and cobalt carbonyls in an organic solvent has been one of the largest chemical processes [1,2]. While the metal carbonyl catalysts exhibit high selectivity for the conversion of ethylene to the desired product, propionaldehyde, the system suffers from two major disadvantages; the requirement of separation of the products from the solvent, an operation which is energy intensive, and the severe environmental problems associated with water pollution.

These problems may be overcome if one could conduct the reaction via a heterogeneous route, however,

up to this point in time no practical catalyst system has been developed. A number of workers have investigated the potential of supported rhodium catalysts for olefin hydroformylation reactions [3–9] and while some improvements in selectivity were observed in the presence of certain promoters, the overall results were still inferior to those achieved in the homogeneous reaction catalyzed by metal carbonyls and complexes [3,6].

We have mounted an investigation designed to test the potential of graphite nanofiber (GNF) supported rhodium catalysts for the ethylene hydroformylation reaction. The objectives of the current work were twofold: (a) To compare the catalytic activity and selectivity of GNF supported rhodium with that displayed by Rh/SiO₂ under the same conditions, and (b) To ascertain the variations in the performance of

* Corresponding author.

the metal particles when supported on different types of GNF materials.

Previous studies of the hydrogenation of simple olefins have demonstrated that dramatic increases in both catalytic activity and selectivity were realized when nickel was supported on highly graphitic nanofibers compared to the performance obtained when the metal was dispersed on more traditional support materials, such as active carbon and γ -alumina [10,11]. Extraordinary high selectivity to crotyl alcohol was also achieved when a Ni/GNF catalyst was used for the gas phase hydrogenation of crotonaldehyde [12]. Since both hydroformylation and hydrogenation involve C=C bond rupture and C–H bond formation [13], it was surmised that a GNF supported metal catalyst may also give rise to high product selectivity during such a reaction.

Graphite nanofibers are a newly developed material produced from the decomposition of selected carbon-containing gases over certain metallic surfaces at temperatures ranging from 400 to 800°C. The solid consists of graphite sheets perfectly arranged in various orientations with respect to the fiber axis, where the degree of crystalline character of the deposited nanofiber is dictated by the chemical nature of the catalyst particle, the composition of the reactant gas and the temperature. One of the most outstanding features is the presence of a large number of edges, which in turn constitute sites that are readily available for chemical reaction or physical interactions [14,15].

Many of the observed variations in the catalytic behavior of nickel on the different types of nanofibers have been attributed to differences in the morphological characteristics of the particles that are dictated on their location sites of the supports. The carbon atoms in the graphite edge regions can adopt one of two arrangements, the so-called “arm-chair” and “zig-zag” conformations. In an attempt to establish whether the active state of nickel is one that is preferentially located on a particular set of edge faces a series of experiments was undertaken in which the nanofibers were pretreated with certain additives that are known to chemically block selected graphite sites. Treatment of graphite with certain phosphorus compounds has been shown to preferentially block “arm-chair” faces, whereas boron selectively substitutes into the “zig-zag” faces [16,17]. When nickel was introduced onto these respective chemically modified nanofibers

the phosphorus containing materials were found to exhibit a similar reactivity pattern to that of the pristine samples. In contrast, incorporation of boron into the GNFs rendered the supported metal system virtually inactive for hydrogenation of olefins. Based on these results, it was tentatively concluded that the active state of nickel was one where the particles were preferentially located on the “zig-zag” faces of the nanofiber structures [18].

2. Experimental

2.1. Materials

Three types of GNFs were selected for this study classified as a “platelet” (P), structure in which the graphite sheets were aligned perpendicular to the fiber axis; a “ribbon-like” (R) form where the sheets were arranged parallel to the fiber axis; and “herring-bone” (H), where the sheets are oriented at an angle to the fiber axis. The GNF-P structures were prepared from the Fe catalyzed decomposition of CO/H₂ at 600°C [19], GNF-R materials were generated from the Fe-Ni catalyzed decomposition of CO/H₂ at 600°C [20] and GNF-H samples from the Fe-Cu catalyzed decomposition of C₂H₄/H₂ at 600°C [21]. The resulting GNFs were demineralized in 1 M hydrochloric acid for a period of 7 days to remove any of the associated metal catalyst particles. The nanofibers were then thoroughly washed in deionized water, dried overnight in air at 110°C and stored until required for use.

The 4 wt.% rhodium supported catalysts used in this investigation were prepared by a standard incipient wetness technique using an alcohol solution of RhCl₃·3H₂O. The catalyst precursor was firstly calcined in air at 250°C for 2 h to convert the metal nitrate to oxide and then reduced in 10% H₂/He at 400°C for 8 h. In the case of the Rh/SiO₂ system, the reduction step was allowed to proceed for 48 h in order to ensure complete transformation of the crystallites to the metallic state. The reduced catalysts were cooled in helium, passivated at room temperature in a 2% CO₂/He mixture for 1 h prior to removal from the reactor.

The gases used in this work, ethylene (99.999%), carbon monoxide (99.99%), hydrogen (99.999%) and helium (99.99%) were obtained from Medical Technical Gases and used without further purification. Silica

(99.5%, surface area $300\text{ m}^2/\text{g}$) was purchased from Strem Chemicals and reagent grade rhodium chloride [$\text{RhCl}_3 \cdot 3\text{H}_2\text{O}$] was supplied by Alfa Products.

2.2. Apparatus and procedures

The catalysis unit used in this investigation was comprised of a quartz flow reactor, fitted with a quartz frit located in the central region of the reactor tube, which was heated with a split vertical tube furnace. The gas flow to the reactor was precisely regulated by the use of MKS mass flow controllers allowing a constant composition of a desired reactant feed to be delivered. Catalyst samples (100 mg) were placed on the quartz frit and the tube was positioned in such a manner that the frit was always in approximately the same point in the reactor. After reduction in a $20\%\text{H}_2/\text{He}$ mixture for 1 h at 350°C , the system was cooled to the desired reaction temperature whilst maintaining this gas flow. Once the desired reaction temperature was attained, the reactant mixture, such as $\text{CO}/\text{H}_2/\text{C}_2\text{H}_4/\text{He}$ (1:1:1:1) was introduced to the reduced catalyst sample at a flow rate of $120\text{ cm}^3/\text{min}$ and the reaction allowed to proceed at temperatures ranging from 180 to 300°C for periods of up to 2 h. The reaction was followed as a function of time by sampling the inlet and outlet gas streams at regular intervals and analyzing the reactants and products by gas chromatography using a 30 m megabore (GS-Q) capillary column in a Varian 3400 GC unit.

The BET surface areas of the various support media were obtained from nitrogen adsorption experiments performed at -196°C with a Coulter Omnisorp 100CX unit. Transmission electron microscopy examinations of the catalyst samples were performed in a JEOL 2000 EXII microscope (point-to-point resolution of this instrument was 0.18 nm). Transmission specimens were prepared by ultrasonic dispersion of a small quantity of a given catalyst in *iso*-butanol and

then applying a drop of the supernate to a holey carbon film. Electron micrographs were taken of several regions of each specimen and the size distribution profiles constructed from measurements of over 250 particles in each system.

3. Results

3.1. Catalyst characterization studies

The N_2 BET surface areas of demineralized samples of each catalyst support material, measured at -196°C are presented in Table 1. Also included in this table are the data for the corresponding supported metal catalysts. It is evident that the surface areas of the demineralized GNFs change as a function of the arrangement of the graphite sheets constituting the various conformations, however, in all cases, these materials exhibit values that are considerably higher than a conventional graphite sample, which is typically $<1.0\text{ m}^2/\text{g}$. It is also apparent that, within experimental error, there are no major modifications in the respective surface areas following the introduction of the metallic phase onto the support media. This finding indicates that the various treatment steps required to generate the dispersed rhodium crystallites do not exert any adverse effects on the structural integrity of the GNF samples.

Examination of the catalyst samples by transmission electron microscopy (TEM) revealed that in all the GNF supported systems, the metal particles tended to accumulate at the edge regions. Close inspection of these specimens showed that the rhodium adopted a thin, hexagonal-shaped morphology. In contrast, when silica was used as the support medium the particles tended to have a more globular appearance. It was apparent from particle size measurements, presented in Fig. 1, that the distribution was significantly broader on the GNF supports than on silica. From

Table 1
BET N_2 surface areas of the various pristine supports and corresponding catalysts

Type of support	Surface area (m^2/g)	Catalyst system	Surface area (m^2/g)
GNF-R	51.5	Rh/GNF-R	55.9
GNF-P	94.3	Rh/GNF-P	139.5
GNF-H	214.8	Rh/GNF-H	212.4
SiO_2	234.4	Rh/ SiO_2	220.2

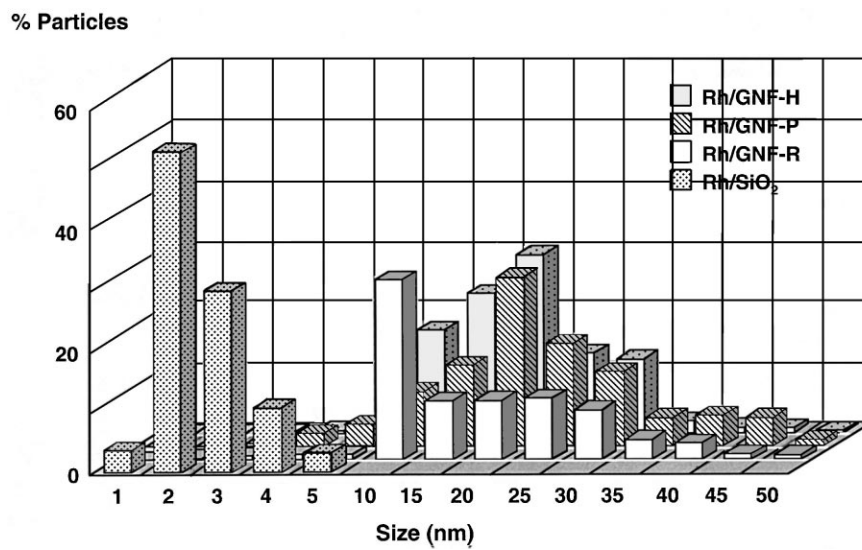


Fig. 1. Particle size distribution of rhodium crystallites dispersed on the four support media prior to reaction in CO/C₂H₄/H₂.

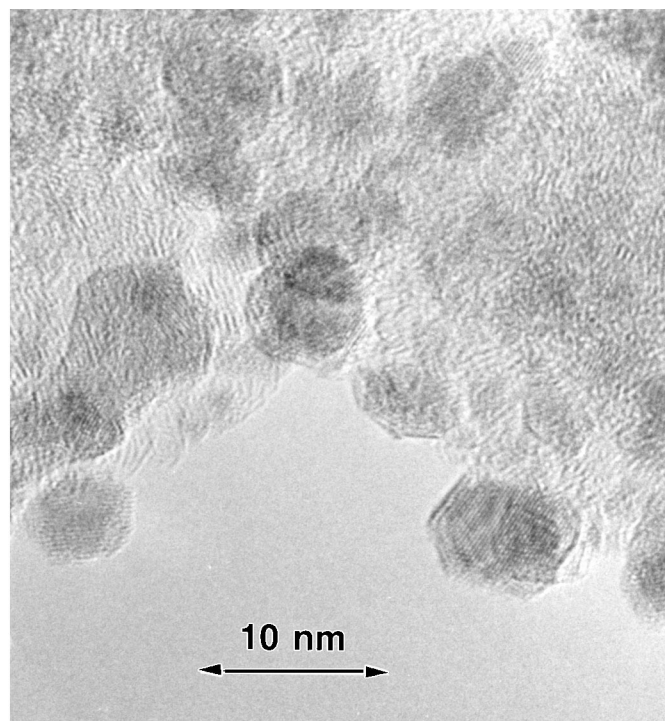


Fig. 2. High resolution transmission electron micrograph showing the hexagonal-shaped appearance of rhodium crystallites located on the edges of a GNF-H support.

these profiles it has been possible to compute the average particle sizes on the various support media as follows: Rh/SiO₂ = 2.6 nm; Rh/GNF-P = 22.6 nm; Rh/GNF-H = 19.1 nm; and Rh/GNF-R = 15.1 nm. Fig. 2 is a high resolution micrograph showing the details of rhodium crystallites located on the edge of a GNF-H support. The highly crystalline hexagonal-shaped particles are thin enough to allow one to distinguish the presence of the lattice fringe images, characteristics that are consistent with the establishment of a strong metal-support interaction. The d-spacing of the metal particles as measured from the negative of this micrograph was 0.222 nm, which can be compared with the literature value of 0.220 nm for Rh₍₁₁₁₎.

These metal particle characteristics also observed on the other GNF supports, however, it was not possible to establish with any degree of certainty whether the formation of such morphological structures was more prevalent one particular type of material than another. Examination of specimens after reaction with a C₂H₄/CO/H₂/He reactant at temperatures up to 300°C revealed that there was no major change in either the average size or shape of the metal particles, indicating that loss of rhodium via carbonyl formation was not occurring to any significant extent.

3.2. Flow reactor studies

The reaction of C₂H₄/CO/H₂/He (1:1:1:1) mixtures with the various supported rhodium catalysts systems was performed at temperatures over the range 180–300°C and analysis of the major products, propionaldehyde (ethylene hydroformylation) and ethane (ethylene hydrogenation) was performed at regular intervals over a 2 h period. In most cases, the reaction reached a steady state after about 10 min on stream. The conversion levels of ethylene were found to be strongly dependent upon the nature of the support material and the reaction temperature as shown in Fig. 3. Inspection of these data indicates that the Rh/SiO₂ system exhibits the highest activity with respect to conversion of the olefin and that the Rh/GNF-P system is the most active of the graphite supported catalysts. It was interesting to find that whilst the activity of the Rh/SiO₂ system exhibited a steady increase as the temperature was raised from 180 to 300°C, that of the corresponding GNF supported metal catalysts remained relatively constant over this temperature range.

It is intriguing to find that while the activity of the GNF supported Rh catalysts are lower than that realized with the Rh/SiO₂ system, the former type of

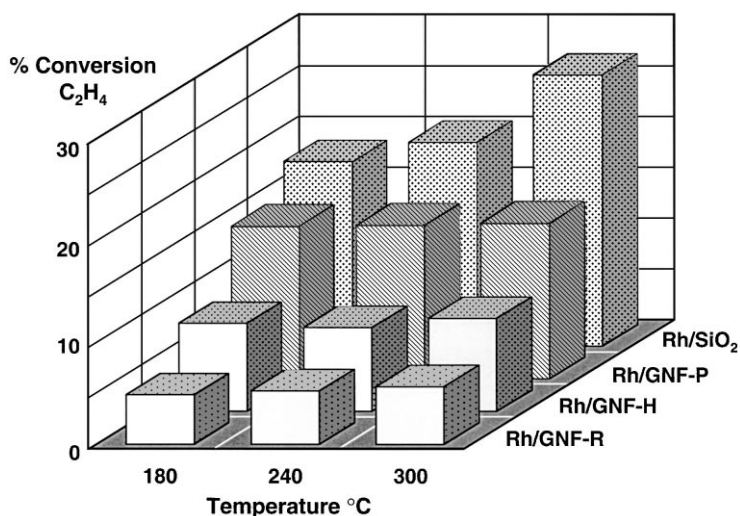


Fig. 3. Percentage conversion of ethylene achieved after 30 min reaction as a function of temperature over rhodium dispersed on the four support media.

Table 2

Percent product distribution from the reaction of CO/C₂H₄/H₂ (1:1:1) over various supported rhodium catalysts after 1 h at 240°C

Catalyst system	CH ₄	C ₂ H ₆	C ₂ H ₅ CHO
Rh/GNF-R	–	2.40	2.31
Rh/GNF-P	–	8.91	6.15
Rh/GNF-H	–	6.35	2.53
Rh/SiO ₂	0.08	21.38	1.42

support materials exert a significant effect on the selectivity pattern. This aspect is highlighted in Table 2, which shows the percent product distribution from a CO/C₂H₄/H₂/He (1:1:1:1) mixture and Fig. 4, a plot showing the percent selectivity towards the desired product propionaldehyde for the various supported Rh catalysts as a function of time at 240°C. The percentage selectivity was calculated from the relationship: propionaldehyde/(ethane+propionaldehyde). The variation in this parameter as a function of reaction temperature is presented in Fig. 5 where it is apparent that the optimum conditions are achieved for all catalyst systems at 240°C with the best performance being exhibited by the Rh/GNF-R catalyst, reaching a level of about 50% selectivity to propionaldehyde.

In a further set of experiments, the reaction temperature was maintained at 240°C while the ratio of the

Table 3

Percent product distribution from the reaction of CO/C₂H₄/H₂ (1:1.5:1) over various supported rhodium catalysts after 1 h at 240°C

Catalyst system	CH ₄	C ₂ H ₆	C ₂ H ₅ CHO
Rh/GNF-R	–	4.36	3.30
Rh/GNF-P	–	10.54	6.49
Rh/GNF-H	–	5.57	3.00
Rh/SiO ₂	0.04	16.06	2.24

reactants was systematically changed. The effect of increasing the concentration of ethylene in the reactant so that ratio of the CO/C₂H₄/H₂/He mixture was (1:1.5:1:0.5) on the selectivity towards propionaldehyde formation is shown as a function of time in Fig. 6 and the percent product distribution from the various catalyst systems is given in Table 3. With the exception of the Rh/GNF-R system, it is apparent that there is a general increase in this parameter.

Fig. 7 and Table 4 show the results of conducting the same set of experiments in the presence of a CO/C₂H₄/H₂/He (1.5:1:1:0.5) reactant mixture where the concentration of CO was increased relative to the other components. In this case the selectivity towards propionaldehyde increased for all the GNF supported rhodium systems, relative to that obtained with an equimolar mixture. On the other hand, the Rh/SiO₂

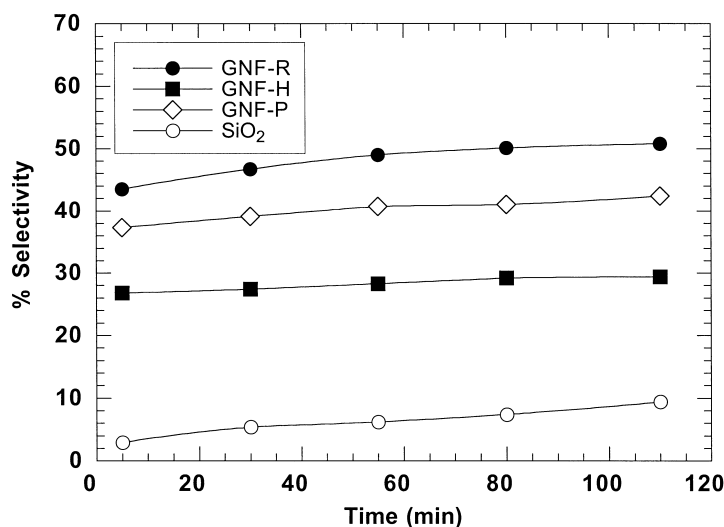


Fig. 4. Percentage selectivity towards propionaldehyde from the interaction of a CO/C₂H₄/H₂/He (1:1:1:1) mixture as a function of time with various supported rhodium catalysts at 240°C.

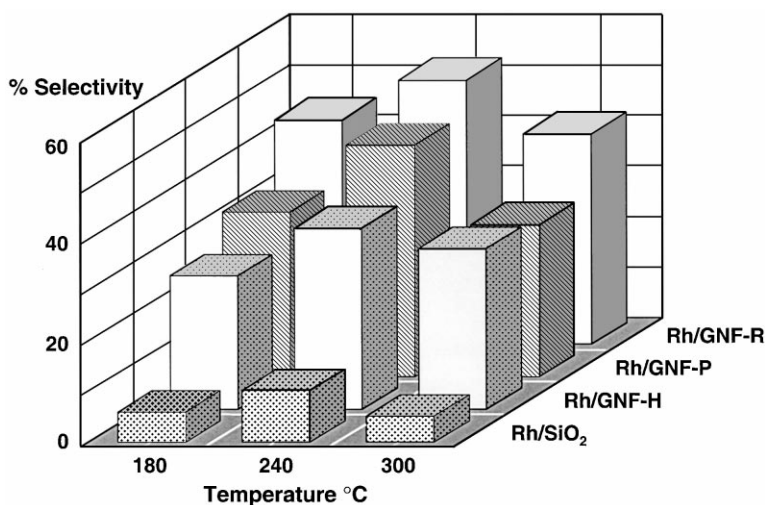


Fig. 5. Selectivity towards propionaldehyde from the interaction of a CO/C₂H₄/H₂/He (1:1:1:1) mixture over various supported rhodium catalysts as a function of reaction temperature.

catalyst did not appear to be sensitive to the change in reaction conditions.

Finally, the suite of catalysts were exposed to a CO/C₂H₄/H₂/He (1:1:1.5:0.5) reactant mixture in which hydrogen was the major component and the data obtained from these experiments is given

in Fig. 8 and Table 5. Under these circumstances, it was found that all the GNF supported rhodium samples exhibited lower selectivity values, whereas once again the Rh/SiO₂ system did not appear to be affected by this modification in reactant composition.

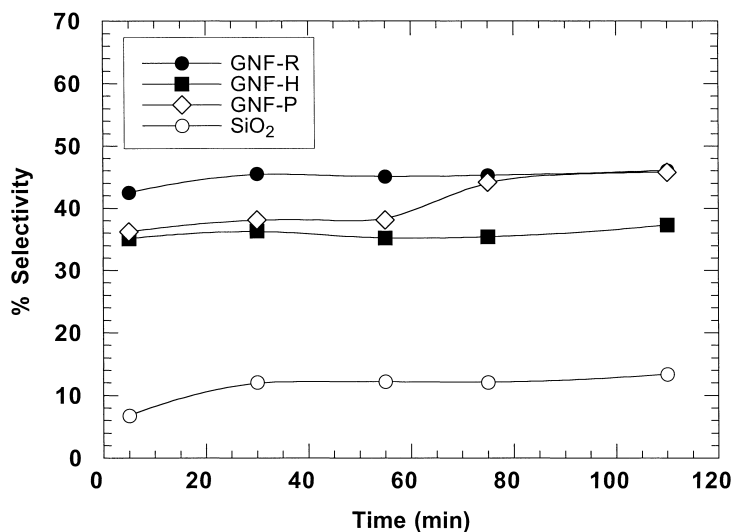


Fig. 6. Percentage selectivity towards propionaldehyde from the interaction of a CO/C₂H₄/H₂/He (1:1.5:1:0.5) mixture as a function of time with various supported rhodium catalysts at 240 °C.

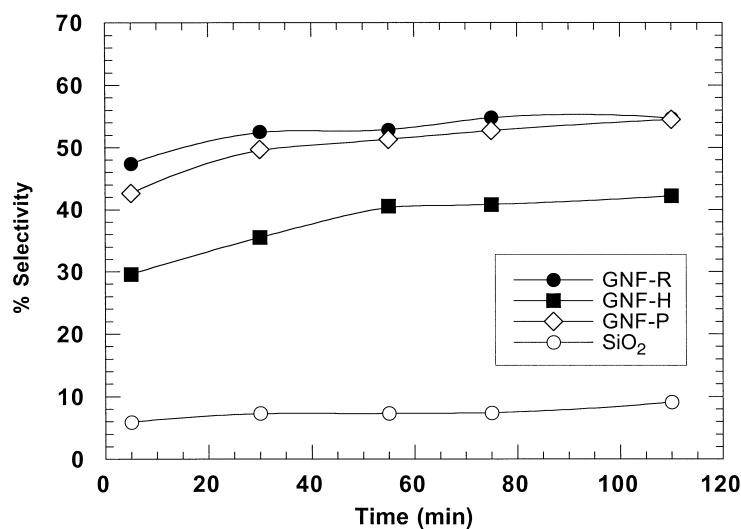


Fig. 7. Percentage selectivity towards propionaldehyde from the interaction of a CO/C₂H₄/H₂/He (1.5:1:1:0.5) mixture as a function of time with various supported rhodium catalysts at 240°C.

Table 4

Percent product distribution from the reaction of CO/C₂H₄/H₂ (1.5:1:1) over various supported rhodium catalysts after 1 h at 240°C

Catalyst system	CH ₄	C ₂ H ₆	C ₂ H ₅ CHO
Rh/GNF-R	–	2.25	2.25
Rh/GNF-P	–	3.47	3.42
Rh/GNF-H	–	2.67	1.81
Rh/SiO ₂	0.10	18.25	1.44

Table 5

Percent product distribution from the reaction of CO/C₂H₄/H₂ (1:1:1.5) over various supported rhodium catalysts after 1 h at 240°C

Catalyst system	CH ₄	C ₂ H ₆	C ₂ H ₅ CHO
Rh/GNF-R	–	4.95	2.48
Rh/GNF-P	–	10.65	4.32
Rh/GNF-H	–	7.40	2.71
Rh/SiO ₂	0.10	18.78	1.82

4. Discussion

Before attempting to rationalize the effect of the support media on the observed catalytic behavior of rhodium, it is important to review the pertinent literature in this area. While there is still conjecture about the precise reaction mechanism, a very plausible explanation for the formation of the major products has been presented by Balakos and Chuang [22]. These workers used a combination of transient isotopic methods and in situ infrared spectroscopy to demonstrate that in the CO/C₂H₄/H₂ reaction with Rh/SiO₂, a C₂H₅ adsorbed species was an intermediate for the formation of both propionaldehyde (hydroformylation) and ethane (hydrogenation). It was claimed that the former product originated from the interaction of

the acyl intermediate with a linear CO molecule, followed by hydrogenation to generate the aldehyde [8].

The current investigation has revealed that when rhodium was dispersed on GNF supports, major differences in the catalytic performance for the ethylene hydroformylation reaction was observed compared to that displayed when the same metal loading was supported on silica. While the catalytic activity, as determined by the percent conversion of ethylene in a given time period, was lower on the Rh/GNF systems than that achieved with the oxide supported catalyst, the selectivity towards the desired product, propionaldehyde, was superior on the former support materials. Furthermore, it was evident that the specific nanofiber structure exerted an impact on the catalytic behavior of the supported rhodium particles with the Rh/GNF-R

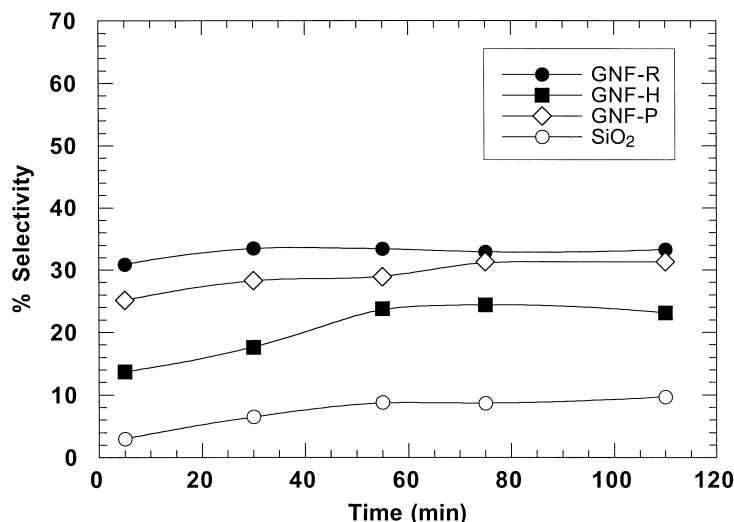


Fig. 8. Percentage selectivity towards propionaldehyde from the interaction of a CO/C₂H₄/H₂/He (1:1:1.5:0.5) mixture as a function of time with various supported rhodium catalysts at 240°C.

system exhibiting the highest selectivity towards propionaldehyde formation under all the conditions used in this investigation.

In order to gain an insight into the factors controlling the influence of these unique types of carbonaceous supports it is necessary to examine the details of their structural architecture. The exposed surfaces of the materials consist of graphite edges where each layer is separated from the next in a uniform manner by a distance of 0.335 nm. The arrangement of carbon atoms at the edges of graphite can be either in a “zig-zag” {1010} or “arm-chair” {1120} form as shown in the schematic diagram (Fig. 9). Both the GNF-P and GNF-H types of materials have surfaces that consist of an equivalent number of “zig-zag” and “arm-chair” sites, thus, giving rise to major differences in the morphological characteristics of the deposited rhodium particles. On the other hand, the surface carbon atom arrangement of the GNF-R material has not been established. Further work using the concept of chemical blocking agents, a method that has been demonstrated to be a very effective means of probing the nature of the exposed edges of GNFs [18] is in progress and will allow us to identify which type of carbon atom arrangements exist in the GNF-R material.

High resolution transmission electron microscopy examinations of the supported rhodium catalysts showed that the particles in contact with the nanofiber edges adopted a set of morphological characteristics that were consistent with the establishment of a strong metal-support interaction. Measurements of the d-spacing of the lattice fringe images of the metal particles indicated that the Rh₍₁₁₁₎ was the predominant crystallographic face. It was significant that these features were not observed when the metal was dispersed on silica.

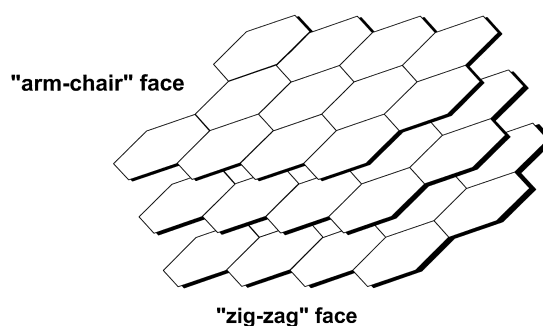


Fig. 9. Schematic representation showing the arrangement of carbon atoms in the “arm-chair” and “zig-zag” prismatic faces of graphite.

While the overriding factor in the attainment of the desired selectivity may be geometric arrangement of rhodium atoms, one must not overlook the possibility that since the GNF are electrically conductive in nature, a property that is directly related to the presence of delocalized π -electrons associated with the basal plane regions of the graphite, it is not unreasonable to expect that electronic perturbations in the metal could be operative. The existence of a significant palladium–carbon interaction was reported by Mojet and co-workers [23] from their studies of noble metals dispersed on carbon fibrils (a material that can be classified as carbon nanofibers). These workers used a X-ray absorption fine structure (XAFS) spectroscopy to examine the state of the catalyst and concluded that palladium species were stabilized on the support by carboxylic groups and the π -electron system of the carbonaceous material.

There are a number of reports demonstrating that the electronic state of surface rhodium atoms is a critical factor in determining catalytic activity and selectivity in reactions involving CO insertion steps into hydrocarbon species [24–27]. Mate and coworkers [28] have demonstrated that during the co-adsorption of CO and ethylene on the $\text{Rh}_{(111)}$ face, the olefin functions as an electron donor whereas CO has the ability to withdraw electrons from the metal surface and this co-operative behavior results in the establishment of a unique interaction between the two types of adsorbed molecules. Other workers [7] have reported that the addition of sodium ions to rhodium was found to exert a major impact on the electronic state of the metal, which was manifested by a increase in the catalytic activity for both hydrogenation and hydroformylation reactions.

When the supported rhodium catalysts were treated in reactant mixtures in the partial pressures of the constituents were systematically changed with respect to each other significant changes in the selectivity towards propionaldehyde were found. Comparison of the data presented in Figs. 4 and 6–8, and Tables 2–5 shows a number of interesting trends. In reactions where ethylene is the major gaseous component (Fig. 6), there is a perceptible increase in the selectivity of Rh/GNF-H, Rh/GNF-P and Rh/SiO₂ towards propionaldehyde formation, whereas the performance of the Rh/GNF-R system appears to be unaffected by this modification in reaction conditions. When the reaction was conducted in a mixture containing excess

CO (Fig. 7), all the Rh/GNF systems exhibited an enhancement in selectivity towards propionaldehyde, whereas the Rh/SiO₂ did show any change in performance from that observed in the equimolar mixture. Finally, when the partial pressure of hydrogen was increased relative to the other reactants, then in this case the selectivity of all the Rh/GNF systems to the desired product decreased, while once again the Rh/SiO₂ catalyst remained insensitive to the change (Fig. 8). A consistent feature in all these experiments is that methane was only found from reactions involving the Rh/SiO₂ catalyst. Furthermore, under the conditions followed in this study, hydrogenation of the adsorbed species to produce ethane is the favored reaction step with all the catalyst systems. These data are to be compared with those obtained by Balakos and Chuang [22] who reported that when the total gas pressure was increased while maintaining the ratios of the various components constant, the rate of hydrogenation was increased and that leading to propionaldehyde decreased.

5. Summary

While the current investigation does not provide any major new insights into the mechanistic aspects of the heterogeneous hydroformylation of ethylene, it has generated some very important information with regard to the impact of the support on the selectivity of this reaction. It has been demonstrated that when rhodium was dispersed on micro-engineered electrically conductive GNF support media the selectivity towards propionaldehyde was significantly enhanced over that achieved with a Rh/SiO₂ catalyst containing the same metal loading. The optimum temperature for the hydroformylation reaction was found to be 240°C, since at this condition one was able to achieve the combination of maximum activity with acceptable selectivity. High resolution transmission electron microscopy examinations the Rh/GNF catalysts revealed that the metal crystallites adopted a distinct faceted morphology in which the (111) faces were preferentially exposed to the gas phase. It is claimed that the nanofibers function as a template for the metal particles which in turn acquire crystallographic characteristics that are not generally encountered with other less ordered support materials. This aspect is

believed to be one of the critical factors in determining the performance of the supported rhodium particles. One must also be aware that since the GNF support is an electrical conductor, there is also the distinct possibility that the metal-support interaction results in the electronic perturbation of the rhodium crystallites and this phenomenon could exert an impact on the catalytic behavior of the system.

Acknowledgements

This work was supported by a grant from the National Science Foundation, Division of Chemical and Transport Systems, no. CTS-9634266.

References

- [1] I. Wender, H.W. Sternberg, W. Orchin, in: P.H. Emmett (Ed.), *Catalysis*, Vol. 5, Reinhold, New York, 1957, p. 73.
- [2] G.W. Parshall, *Homogeneous Catalysis — The Applications and Chemistry by Soluble Transition Metal Complexes*, Wiley, New York, 1981, p. 85.
- [3] M. Ichikawa, *J. Catal.* 59 (1979) 67.
- [4] M.E. Davis, E. Rode, D. Taylor, B.E. Hanson, *J. Catal.* 86 (1984) 67.
- [5] R.J. Davis, J.A. Rossin, M.E. Davis, *J. Catal.* 98 (1986) 477.
- [6] N. Takahashi, A. Mijin, H. Suematsu, S. Shinohara, H. Matsuoka, *J. Catal.* 117 (1989) 348.
- [7] S. Natio, M. Tanimoto, *J. Catal.* 130 (1991) 106.
- [8] S.S.C. Chuang, S.I. Pien, *J. Catal.* 135 (1992) 618.
- [9] G. Srinivas, S.S.C. Chuang, *J. Catal.* 144 (1993) 131.
- [10] A. Chambers, T. Nemes, N.M. Rodriguez, R.T.K. Baker, *J. Phys. Chem.* 102 (1998) 2251.
- [11] C. Park, R.T.K. Baker, *J. Phys. Chem.* 102 (1998) 5168.
- [12] F. Salman, C. Park, R.T.K. Baker, *Catal. Today* 53 (1999) 385.
- [13] H. Arai, H. Tominaga, *J. Catal.* 75 (1982) 188.
- [14] N.M. Rodriguez, *J. Mater. Res.* 8 (1995) 625.
- [15] N.M. Rodriguez, A. Chambers, R.T.K. Baker, *Langmuir* 11 (1995) 3862.
- [16] S.G. Oh, N.M. Rodriguez, *J. Mater. Res.* 8 (1993) 2879.
- [17] N.M. Rodriguez, R.T.K. Baker, *J. Mater. Res.* 8 (1993) 1886.
- [18] C. Park, R.T.K. Baker, *J. Phys. Chem.* 103 (1999) 2453.
- [19] N.M. Rodriguez, M.S. Kim, R.T.K. Baker, *J. Catal.* 144 (1993) 93.
- [20] C. Park, N.M. Rodriguez, R.T.K. Baker, *J. Catal.* 169 (1997) 212.
- [21] N. Krishnankutty, N.M. Rodriguez, R.T.K. Baker, *Catal. Today* 37 (1997) 295.
- [22] M.W. Balakos, S.S.C. Chuang, *J. Catal.* 151 (1995) 253.
- [23] B.L. Mojet, M.S. Hoogenraad, A.J. van Dillen, J.W. Geus, D.C. Koningsberger, *J. Chem. Soc., Faraday Trans.* 93 (1997) 4371.
- [24] W.M.H. Sachtler, M. Ichikawa, *J. Phys. Chem.* 90 (1986) 4752.
- [25] P.R. Watson, G.A. Somorjai, *J. Catal.* 72 (1981) 347.
- [26] D.G. Castner, R.L. Blackadar, G.A. Somorjai, *J. Catal.* 66 (1980) 257.
- [27] M. Kawai, M. Uda, M. Ichikawa, *J. Phys. Chem.* 89 (1985) 1654.
- [28] C.M. Mate, C.T. Kao, G.A. Somorjai, *Surf. Sci.* 206 (1988) 145.